Enhanced grain refinement and microhardness by hybrid processing using hydrostatic extrusion and high-pressure torsion

P. Bazarnik, Y. Huang, M. Lewandowska, T.G. Langdon

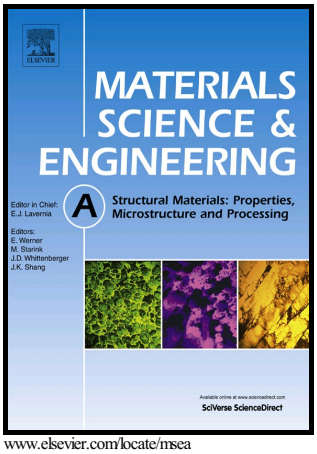

www.elsevier.com/locate/msea

PII: S0921-5093(17)31604-0
DOI: https://doi.org/10.1016/j.msea.2017.12.007
Reference: MSA35849

To appear in: *Materials Science & Engineering A*

Received date: 28 August 2017
Revised date: 23 November 2017
Accepted date: 4 December 2017

Cite this article as: P. Bazarnik, Y. Huang, M. Lewandowska and T.G. Langdon, Enhanced grain refinement and microhardness by hybrid processing using hydrostatic extrusion and high-pressure torsion, *Materials Science & Engineering A,* https://doi.org/10.1016/j.msea.2017.12.007

Submission to Materials Science and Engineering A (August 2017)

Enhanced grain refinement and microhardness by hybrid processing using hydrostatic extrusion and high-pressure torsion

P. Bazarnik[a,*], Y. Huang[b], M. Lewandowska[a], T.G. Langdon[b,c]

[a]Warsaw University of Technology, Faculty of Materials Science, Woloska 141, 02-507, PL

[b]Materials Research Group, Faculty of Engineering and the Environment, University of Southampton, Southampton SO17 1BJ, UK

[c]Departments of Aerospace & Mechanical Engineering and Materials Science, University of Southern California, Los Angeles, CA 90089-1453, USA

Abstract

An investigation was conducted to examine the microstructure and mechanical properties of an Al-5483 aluminium alloy subjected to a hybrid severe plastic deformation (SPD) process consisting of hydrostatic extrusion (HE) followed by high-pressure torsion (HPT) for up to 10 revolutions. The results are compared with those for samples processed separately by HE or by HPT. Microhardness measurements were taken on cross-sectional planes of the HE billets and on the HPT disks and in addition the microstructures were examined using transmission electron microscopy. The results demonstrate that the hybrid process of HE+HPT induces additional grain refinement when compared with HPT with average grain sizes of ~60 and 90 nm, respectively. Also, a significantly higher fraction of high-angle grain boundaries (HAGBs) was present after HE+HPT and the beneficial role of HE pre-processing was also apparent in the microhardness measurements. After the hybrid process, the microhardness saturated at Hv ≈ 255 which is higher than after either HPT (Hv ≈ 235) or HE (Hv ≈ 160). A linear Hall-Petch relationship was maintained for coarse-grained and SPD-processed samples with high fractions of HAGBs (above 70%) while samples with higher fractions of low-angle grain boundaries showed a significant deviation from linearity.

Keywords: Combinations of SPD, Grain boundary misorientation angles, High-pressure torsion, Hydrostatic extrusion, Microhardness, Ultrafine grains.

*Corresponding author: Piotr Bazarnik (p.bazarnik@inmat.pw.edu.pl)

1. Introduction

The processing of metallic materials by severe plastic deformation (SPD) has attracted special interest since it offers an opportunity for the fabrication of ultrafine-grained (UFG) and nanocrystalline (NC) metals and alloys with superior mechanical properties [1,2]. A number of SPD methods were developed, such as high-pressure torsion (HPT) [3], equal-channel angular pressing (ECAP) [4], accumulative roll bonding (ARB) [5] and hydrostatic extrusion (HE) [6]. Among these methods, HPT is regarded as the most promising in terms of producing structures with the smallest grain sizes in various metallic materials [7-12] and the highest fraction of grain boundaries (GB) having high angles of misorientation [13]. In practice, HPT is ideal for achieving UFG and NC structures because of its ability to generate extremely high strains.

However, a true NC structure is difficult to achieve in some metallic materials when processing via a single SPD method even when extremely high strains, as in HPT, are applied to the samples [14]. Published data show that most metallic materials processed by SPD techniques exhibit a similar limitation in which a minimum grain size is achieved in the so-called saturation effect [15]. The concept of saturation is described as a certain level of applied strain above which it is no longer possible to achieve any further grain fragmentation and strengthening. Limitations in the grain refinement have attracted much attention recently but the physical process underlying this phenomenon is not yet understood. In some research the saturation condition is described as a state in which the density of the generated dislocations is so high that their movement is blocked on all available slip systems [16,17]. At this point, from a thermo-mechanical point of view, dislocation annihilation and recovery processes start to play a crucial role and an equilibrium is reached between work hardening and recovery processes. Some published data show that further enhancements of strength may be obtained by changing the deformation route [13,16-26]. Nevertheless, the concept of combining different SPD methods in a hybrid technique is relatively new and only partially explored. Some data suggest that this phenomenon is associated with a change in the deformation system, for example by initiating dislocation movement on new slip systems in accordance to the changes in the stress-strain conditions, thereby producing a further grain size reduction [17]. The use of hybrid SPD techniques was proven to be very beneficial using low strain SPD techniques [27]. However, since it is known that the high strain procedure of HPT processing is the most effective technique for obtaining true NC structures in Al-Mg alloys [28-31], it remains unclear whether this minimum grain size may be affected by any preliminary processing that is conducted prior to HPT.

The concept of combining HPT processing with other SPD techniques was undertaken in only in a small number of reports focusing mainly on the use of ECAP prior to HPT [13,16-18,20]. However, even among these results there are some contradictions regarding the beneficial influence of using hybrid processing. For example, the use of ECAP and HPT on a large group of metallic samples, including pure titanium [20], nickel [22], copper [17], Cu 0.1Zr [13] and an Al-7075 alloy [18,25,26], was shown to introduce additional grain refinement and an increase of strength in these materials. By contrast, in experiments on pure niobium [16] the use of a hybrid technique gave no significant change in the microstructure and mechanical properties when comparing with samples processed only by HPT [32]. The results from this latter study suggest, therefore, that the saturation level is an inherent feature of each material and accordingly that it cannot be changed through any manipulations of the stress-strain state.

Based on this apparent dichotomy, the present research was initiated to examine the nature of the saturation phenomenon in an aluminium 5483 alloy. Previous studies showed that this material exhibits a potential for achieving saturation conditions when processing only by HPT [30]. Accordingly, the objective of this research was to determine whether it is possible to produce samples with even smaller grain sizes, and thus to improve the mechanical properties of the alloy, by using a new type of hybrid SPD processing in which HE is followed by HPT. Specifically, the aim of this work was to provide an understanding of microstructural evolution when the deformation mode is changed and to further examine the impact of this evolution on the mechanical properties.

2. Experimental material and procedures

The material investigated in this study was a commercial aluminium 5483 alloy containing, in wt. %, 5% Mg and 1% Mn and supplied in the form of rods with a diameter of 50 mm and lengths of ~1000 mm. A two-step hybrid processing procedure was undertaken. The first step was HE with a diameter reduction to 10 mm. The equivalent strain in HE is given by the equation (1):

$$\varepsilon = 2ln\left(\frac{d'}{d''}\right) \qquad (1)$$

where d' is the initial diameter of the rod and d'' is the exit diameter. The equivalent strain after the HE process was at a level of ~3.2. The extruded rods were cut perpendicular to their longitudinal axes to provide a series of disks with diameters of 10 mm and thicknesses of ~0.8 mm. These disks were processed at room temperature using quasi-constrained HPT [33] with

a constant pressure of 6.0 GPa and a rotation speed of 1 rpm. Disks were torsionally strained through total numbers of revolutions, N, of 1/4, 1/2, 1, 3, 5, 7 and 10. The equivalent von Mises strain, ε_{eq}, achieved in HPT is given by the relationship [34]

$$\varepsilon_{eq} = \frac{2\pi N r}{h\sqrt{3}} \qquad (2)$$

where N is the number of turns, r is the radial distance measured from the disk centre and h is the thickness (or height) of the sample. It follows from eq. (2) that the strain varies across the disk and reaches zero at the disk centre where $r = 0$ and this suggests that the microstructure, as well as the microhardness distributions, will be extremely inhomogeneous across the disks.

All samples were polished with abrasive paper and then microhardness measurements were taken on polished surfaces using an FM-300 microhardness tester. These measurements were taken under a load of 100 g with a dwell time of 10 s. The values of the Vickers microhardness, Hv, were recorded for each disk along a selected diameter with a separation between points of 0.3 mm.

Microstructural characterizations were performed for all samples. These observations were conducted using transmission electron microscopy (TEM) with a JEOL 1200 operating at an accelerating voltage of 120 kV. The microstructure in the HE-processed sample was examined in two orthogonal planes corresponding to the cross-sectional and longitudinal sections to the extrusion direction. The structure in samples after HE+HPT processing was studied in the disk plane at the centre and edge areas. In order to study the evolution of the microstructure resulting from the changes in the deformation mode, thin lamellae for TEM studies were cut from the sample processed with a quarter of one revolution in the region near the centre of the disk. These samples were prepared using a focussed ion beam (FIB) technique with a Hitachi NB5000 microscope following the procedure described in detail in an earlier report [35]. All microstructures were evaluated quantitatively using a computer-aided image analyzer. The grain sizes were described in terms of the equivalent grain diameter, d_{eq}, defined as the diameter of a circle with a surface area equal to the surface area of the grain.

The GB misorientations were determined from the disk planes using Kikuchi diffraction patterns obtained for adjacent grains with convergent beam electron diffraction (CBED) in a high resolution scanning transmission electron microscope (STEM). Diffraction images were taken from neighbouring grains with an Hitachi HD 2700 microscope and then processed using a KILIN program to calculate the crystallographic orientations of individual grains and the misorientations across the GBs. The data are presented in the form of the average GB

misorientation angle (E(θ)) and the fraction of high-angle grain boundaries (HAGBs), where the HAGBs are defined as boundaries having misorientations of more than 15°.

Finally, the results obtained from this study were compared with data obtained on the same material processed only by HPT and reported earlier [30].

3. Experimental results

3.1. Microstructure characteristics after HE and HE+HPT

Fig. 1 shows the microstructure images (cross-section and longitudinal section) for the sample processed by HE to a final diameter of 10 mm ($\varepsilon \approx 3.2$). The microstructure after HE is very complex when taking into account the grain size and GB characteristics. TEM studies from the cross-sectional plane complemented with selected area electron diffraction (SAED) showed that the microstructure after HE processing may be divided into two characteristic types: regions with large undeformed grains having micrometer diameters and increased densities of dislocations (Fig. 1a) and regions where there was clear evidence for grain refinement (Fig. 1b). The average grain size for this refined region was at the level of ~300 nm. On the longitudinal section, the GB and dislocation structures were oriented in the direction of hydrostatic extrusion, thereby creating a characteristic fibrous morphology (Fig. 1c) [27].

Due to the large microstructural inhomogeneity in the extruded sample, it was not possible to perform a quantitative analysis of the GB misorientation angles using the CBED technique. Nevertheless, TEM observations indicated that the sample had a high density of dislocation structures and dislocation boundaries which suggests that low-angle grain boundaries (LAGBs) probably dominate in this sample.

Further HPT processing caused significant microstructural changes in the HE-processed samples. Fig. 2 shows representative TEM images supplemented with SAED patterns, recorded near the edges and centers of disks processed for (a,e) HE+HPT 1/2 turn, (b,f) HE+HPT 1 turn, (c,g) HE+HPT 5 turns and (d,h) HE+HPT 10 turns. The quantitative analyses of the grain sizes for all samples processed using the hybrid procedure are summarized in Table 1. For comparison purposes, Table 1 also includes data from earlier research for samples processed only by HPT [30]. The analysis shows that there is a very significant refinement of the microstructure when the HE is followed by additional processing by HPT. The grain size measurements showed that the average grain size at the edge was reduced to ~150 nm after only 1/4 turn and further straining led to additional grain refinement such that after 10 revolutions the grain size was measured as ~60 nm. It should be noted that

the average grain size for the samples processed only by HPT was on average ~10-20% larger than when processing using the hybrid technique [11,30].

The use of hybrid processing has also a strong impact on the evolution of the microstructure in the central regions of the disks. A combination of HE and 1/2 turn of HPT gave significant microstructural refinement also in the central part of the disk (Fig. 2e) and the grains were reasonably equiaxed with an average grain size of the order of ~720 nm. This contrasted strongly with the results obtained for samples processed only by HPT [30] where there was no measurable grain refinement in the central region until reaching one HPT revolution. Moreover, further straining resulted in an homogenization of the microstructure in the central parts of the disks and additional grain refinement (Fig. 2h). The average grain size in the central part of the disk after HE+HPT through 10 turns was at the level of ~100 nm and this compares with ~200 nm for the sample processed only by HPT for 10 revolutions. It should be noted that the grain size in the central region is only slightly larger than in the outer parts of the disk (~60 nm) and this indicates a microstructure after 10 revolutions that is reasonably homogenized in terms of grain size.

The present data are not sufficient to clearly determine the mechanism dominating the occurrence of additional grain refinement during hybrid processing. Accordingly, thin lamellae for TEM observations were cut by FIB from the sample processed at 1/4 HPT turn near the centre of the disk (approximately 0.2 mm from the centre) in the cross-sectional plane and representative images from this region are presented in Fig. 3. It is apparent from these images that the fibrous microstructure typical of HE is transformed during the HPT processing. Specifically, the microstructure evolves in accordance with the geometrical effect of strain so that it is possible to observe a number of dislocation bands oriented in the direction of the anvil rotation which intersects the dislocation structures formed during HE processing. Furthermore, the formation of new LAGBs and new grains (Fig. 3 b and c) can be observed in the structure. Therefore, it is concluded that additional grain refinement and an increased fraction of HAGBs may be attained by using hybrid SPD processing where this is achieved due to the initiation of new slip systems according to the change in the stress state and the much higher strain accumulated during HPT.

The distributions of GB misorientations angles are shown in Fig. 4 for samples processed through HE and HPT for 1/2, 1, 5 and 10 turns with at least 150 boundaries examined in each sample. For comparison purposes, Table 2 was prepared to include other parameters such as the average GB misorientation angle and the fraction of HAGBs together with data from earlier work for the same alloy processed only by HPT [30]. It is readily apparent from Fig. 4

and Table 2 that there is a significant difference in the distributions of the misorientation angles between samples processed by the hybrid process and those processed only by HPT. Specifically, the fraction of HAGBs in each sample processed in the hybrid process is larger than in the corresponding samples after processing only by HPT and this fraction reaches a maximum of ~90% after HE+HPT for 10 turns. Moreover, the fraction of HAGB after processing by HE+HPT for 1 revolution reaches a similar level (~80%) as in the sample after 10 HPT revolutions. Also, the average misorientation angle increases with the number of revolutions and these values are higher for samples processed using the hybrid SPD technique. The results therefore confirm that the use of hybrid techniques tend to promote the formation of HAGBs. A similar tendency for an evolution towards higher misorientations was observed earlier in an aluminium 7075 alloy processed by ECAP + HPT [18].

3.2.Microhardness after HE and HE+HPT

Measurements of the Vickers microhardness, Hv, were carried out along the diameter of each HPT disk and the results are plotted in Fig. 5. All Hv measurements were taken on polished planes in the mid-sections of the disks to avoid any influence of a gradation of hardness through the thickness [9-11,30,36,37]. The plot also shows the microhardness distribution for samples in the as-received condition and after HE to a diameter of 10 mm. Inspection of Fig. 5 reveals that HE processing ($\varepsilon \approx 3.2$) leads to an increase in the microhardness from the level of ~90 Hv for the as-received condition to ~125 Hv. Nevertheless, the microhardness values are highly inhomogeneous and it is apparent that there are numerous drops in the microhardness values across the rod diameter. This behaviour is due to the high microstructural inhomogeneity in the sample as shown in Fig. 1.

The use of hybrid processing leads to a further increase in the hardness values and the results follow the typical strengthening behaviour described elsewhere [38,39]. For low numbers of revolutions up to 1 turn, there are high microhardness values in the peripheral regions and a gradual decrease towards the centres of the disks. An increase in the numbers of revolutions leads to further strengthening and a general homogenization of hardness across the disk. In general, such strengthening behaviour is consistent with the results reported in earlier research for samples processed only by HPT [11,30,40] but nevertheless close inspection reveals some differences in the microhardness behaviour. For example, the areas of the central inhomogeneous regions in samples prepared by the hybrid process are smaller than in the samples processed only by HPT. Moreover, the minimum microhardness values in the samples processed with a small number of revolutions, as in HE+HPT 1/4, 1/2 and 1 revolution with Hv = 130, 135 and 140, respectively, are higher than for the extruded state

where Hv ≈ 125 while in the HPT samples the microhardness values oscillate near the initial condition up to one revolution.

In order to investigate the effect of the hybrid SPD processing on the evolution of microhardness in the Al-5483 alloy, the results were compared directly with data reported earlier only for HPT [30]. Fig. 6 shows the average microhardness for both processing conditions as a function of numbers of revolutions. It is apparent from this plot that the values of the microhardness for the HE+HPT samples are consistently higher by ~25 Hv than for the samples processed only by HPT. A similar behaviour was observed also in an aluminium 7075 alloy where samples processed by ECAP + HPT also exhibited microhardness values that were higher than those obtained using only the HPT processing [18].

In addition, after larger numbers of turns the central region also undergoes significant strengthening. In the samples processed using the hybrid SPD technique a reasonable level of homogeneity was achieved throughout the disk processed through 7 revolutions whereas in processing only by HPT such behaviour was observed only after 10 revolutions. To study the saturation effect [8] in the samples processed by HE+HPT, the experimental microhardness points from Fig. 5 were plotted in Fig. 7a against the equivalent strain calculated using eqs 1 and 2. Thus, the datum points in Fig. 7a are in reasonable agreement and fall around the solid line. In the early stages of HPT, the hardness values rise very rapidly with the accumulating strain but ultimately there is no significant further increase at equivalent strains above ~50 and thereafter the microhardness values become essentially saturated at Hv ≈ 255 at high strains. The same type of plot was constructed in Fig. 7b for samples processed only by HPT using data from the earlier investigation [30]. All points in Fig. 7b again scatter around a single line but the saturation condition in this case were obtained at a higher value of strain of ~150 and the saturation hardness was Hv ≈ 235. It is apparent form Fig. 7 that the equivalent strain associated with Hv saturation was lower for HE+HPT than when processing only by HPT.

4. Discussion

4.1. The significance of hybrid processing on the evolution of microhardness and microstructures

. In this work the HE processing of an aluminium 5483 alloy with a diameter reduction from 50 to 10 mm led to the formation of a bimodal structure as shown in Fig. 1 with highly elongated grains having high aspect ratios and an average grain size in the refined regions of ~300 nm. Additional processing by HPT reduced the grain size to ~100 nm in the centre of the disk and ~60 nm near the edge after 10 revolutions, as shown in Fig. 2d,h. This result is

reasonable because the microstructure is not in the saturation condition after HE processing. Nevertheless, the grain sizes measured in the samples obtained in the hybrid process were smaller than those reported earlier when processing only by HPT and the microstructures were also more uniform along the sample diameter [11,30]. It is apparent from Table 2 that the aluminium 5483 alloy processed by a hybrid technique has a significantly larger fraction of HAGBs by comparison with the alloy processed only by HPT. Thus, the present results show that the imposition of additional pre-deformation by HE increases the fraction of HAGBs to ~93% whereas in the samples initially processed only by HPT the value was only ~80% after 10 turns. Furthermore, the microstructure in the central regions evolved more quickly when HPT was preceded by HE.

The significant grain refinement in the samples processed by HE+HPT is also reflected in the microhardness measurements. Furthermore, the present investigation reveals a clear difference between the saturation microhardness values achieved in the Al-5843 alloy after the two different SPD processing conditions of HE+HPT and HPT. For HE+HPT the microhardness saturates at ~255 Hv above equivalent strains of ~50 whereas when processing only by HPT the saturation occurs at a lower value of microhardness of ~235 Hv but at a higher equivalent strain of ~150 [30]. All of these results are consistent and they show that a combination of HE and HPT produces samples with smaller average grain sizes, higher fractions of HAGBs and higher hardness values at the saturation level compared with processing only by HE or HPT [27,30].

4.2. The significance of GB characteristics on the Hall–Petch relationship in HE+HPT hybrid processing

The hybrid SPD processing used in these experiments demonstrates the advent of significant grain refinement to ~60 nm in the aluminium 5483 alloy as shown in Fig. 2 and Table 1. The refined microstructure exhibits improved hardness and tends towards homogeneity above 7 turns with a measured hardness across the disk of Hv ≈ 255 Hv as shown in Fig. 5. Such a significant increase in hardness may be explained by Hall-Petch (H-P) strengthening [41,42] as given by the following relationship which is reformulated in terms of hardness to give

$$H = H_0 + k_H d^{-1/2} \quad (3)$$

where H is the hardness and H_0 and k_H are material constants.

To further check on the applicability of the H-P relationship for the aluminium 5483 alloy prepared using a hybrid process, the microhardness values obtained at the edges of the disks

were plotted in Fig. 8 as a function of $d^{-1/2}$ where d is the grain size together with datum points obtained from the same alloy with larger coarser grain sizes [11,27,30]. In addition, the plot includes experimental datum points from an earlier report for an Al-5Mg alloy processed only by HPT [30].

By analysing these results, it is apparent that there is a clear difference in the distributions of the experimental points between the samples obtained in hybrid (HE + HPT) and HPT processing. Thus, the experimental points for samples processed by the hybrid procedure are mutually consistent for the entire range of revolutions and they fit into a linear H-P relationship. On the other hand, in the samples processed only by HPT there is a marked deviation in the H-P relationship for samples processed through a small number of revolutions as, for example, below 1 turn. Such differences in the locations of individual points for the HE+HPT and HE samples suggests that, besides the grain size, there are secondary factors which may also affect the mechanical properties after SPD processing. For example, it has been suggested that the character of the GB may play a crucial role in the tailoring of mechanical properties [43-45]. It is well established that slip transfer through LAGBs is much easier by comparison with HAGBs and therefore they represent weaker barriers for the movement of lattice dislocations. This approach may be expressed in a modified H-P relationship which takes into account the character of individual GB [44]

$$\sigma = \sigma_0 + [M\alpha G\sqrt{3b\theta_{LAGB}(1-f)} + k\sqrt{f}]d^{-1/2} \quad (4)$$

where f is the fraction of HAGBs, M is the Taylor factor, α, k and σ_0 are material constants, G is the shear modulus, θ_{LAGB} is the average misorientation angle of the LAGBs and b is the Burgers vector. It was shown that the values calculated using this approach are in good agreement with experimental results [11,30,43,46-48]. Furthermore, the applicability of this model is also confirmed in the present work because the datum points corresponding to samples processed only by HPT with a small numbers of turns tend to lie below the trend line in Fig. 8 and these samples will have a higher fraction of LAGBs. On the other hand, the samples obtained in the hybrid processing exhibit an increased fraction of HAGBs as shown in Table 2 even when the processing is conducted through a small number of revolutions. This confirms that the observed differences in the positions of the experimental points are consistent with the modified H-P relationship and indicates that the character of the GBs

formed in the SPD processing may have a significant influence on the final mechanical properties of the material.

5. Summary and conclusions

1. A commercial aluminium 5483 (Al-5Mg) alloy was processed by HE and HPT for various amounts of torsional straining between 1/4 and 10 turns. TEM observations show a bimodal structure after HE processing with highly elongated structure in a longitudinal section and a significant grain size reduction after processing through a combination of HE+HPT. The microstructure evolves with torsional straining so that there is not only a continuous reduction in the average grain size but also an increase in the fraction of HAGBs.

2. It is demonstrated that the initial pre-processing by HE gives a significant advantage in achieving grain size reduction when compared with processing only by HPT. The phenomenon of additional grain refinement in a hybrid process is explained as the effect of the change in the stress state which initiates dislocations slip in new slip systems.

3. The microhardness values saturate at ~255 Hv for the hybrid HE+HPT process and this is significantly higher than in the samples processed only by HPT. In addition, the saturation condition is obtained at lower strains (~50) for the samples processed by HE+HPT by comparison with the samples processed only by HPT (~150).

4. The results are summarised in the form of a Hall-Petch plot and they show a linear correlation between samples having high fractions of HAGBs. By contrast, a high scatter from the linear correlation is observed in samples where LAGBs are dominant in the microstructure.

Acknowledgements

The HE processing was carried out at the Institute of High Pressure Physics of the Polish Academy of Sciences. This research was financed by the National Science Centre, Poland, within the projects: PRELUDIUM 7 “Microstructure influence on properties in ultra-fine grained aluminium alloy 5483” under Grant Agreement No. 2014/13/N/ST8/01661 and project ETIUDA 3 No. UMO-2015/16/T/ST8/00160. Two of the authors were supported by the European Research Council under ERC Grant Agreement No. 267464-SPDMETALS (YH and TGL).

References

[1] R.Z Valiev, R.K Islamgaliev, I.V Alexandrov, Bulk nanostructured materials from severe plastic deformation, Prog. Mater. Sci. 45 (2000) 103-189.

[2] R.Z. Valiev, Y. Estrin, Z. Horita, T.G. Langdon, M.J. Zehetbauer, Y.T. Zhu, Producing bulk ultrafine-grained materials by severe plastic deformation, JOM 58(4) (2006) 33-39.

[3] A.P. Zhilyaev, T.G. Langdon, Using high-pressure torsion for metal processing: Fundamentals and applications, Prog. Mater. Sci. 53 (2008) 893-979.

[4] R.Z. Valiev, T.G. Langdon, Principles of equal-channel angular pressing as a processing tool for grain refinement, Prog. Mater. Sci. 51 (2006) 881-981.

[5] Y. Saito, N. Tsuji, H. Utsunomiya, T. Sakai, R.G. Hong, Ultra-fine grained bulk aluminium produced by Accumulative Roll-Bonding (ARB) process, Scr. Mater. 39 (1998) 1221–1227.

[6] M. Lewandowska, H. Garbacz, W. Pachla, K.J. Kurzydlowski, Hydrostatic extrusion and nanostructure formation in an aluminium alloy, Solid State Phenom. 101-102 (2005) 65–69.

[7] A.P. Zhilyaev, B.K. Kim, G.V. Nurislamova, M.D. Baró, J.A. Szpunar, T.G. Langdon, Orientation imaging microscopy of ultrafine-grained nickel, Scr. Mater. 46 (2002) 575-580.

[8] F. Wetscher, B. Tian, R. Stock, R. Pippan, High pressure torsion of rail steels , Mater. Sci. Forum 503–504 (2006) 455-460.

[9] A. Loucif, R.B. Figueiredo, T. Baudin, F. Brisset, R. Chemam, T.G. Langdon, Ultrafine grains and the Hall–Petch relationship in an Al–Mg–Si alloy processed by high-pressure torsion, Mater. Sci. Eng. A 532 (2012) 139-145.

[10] A.T. Krawczynska, M. Lewandowska, R. Pippan, K.J. Kurzydlowski, The effect of high pressure torsion on structural refinement and mechanical properties of an austenitic stainless steel, J. Nanosci. Nanotechnol. 13 (2013) 3246-3249.

[11] P. Bazarnik, B. Romelczyk, Y. Huang, M. Lewandowska, T.G. Langdon, Effect of applied pressure on microstructure development and homogeneity in an aluminium alloy processed by high-pressure torsion, J. Alloy. Compd. 688, (2016) 736-745.

[12] Y. Huang, S. Sabbaghianrad, A.I. Almazrouee, K.J. Al-Fadhalah, T.G. Langdon, The significance of self-annealing at room temperature in high purity copper processed by high-pressure torsion, Mater. Sci. Eng. A 656 (2016) 55-66.

[13] J. Wongsa-Ngam, M. Kawasaki, T.G. Langdon, A comparison of microstructures and mechanical properties in a Cu-Zr alloy processed using different SPD techniques, J. Mater. Sci. 48 (2013) 4653–4660.

[14] R. Pippan, S.G. Scheriau, A. Taylor, M. Hafok, A. Hohenwarter, A. Bachmaier, Saturation of Fragmentation During Severe Plastic Deformation, Annu. Rev. Mater. Res. 40 (2010) 319–343.

[15] A. Bachmaier, M. Hafok, R. Pippan, Rate Independent and Rate Dependent Structural Evolution during Severe Plastic Deformation, Mater. Trans. 51 (2010) 8-13.

[16] V.V. Popov, E.N. Popova, A.V. Stolbovskiy, Nanostructuring Nb by various techniques of severe plastic deformation, Mater. Sci. Eng. A 539 (2012) 22-29.

[17] N.D. Stepanov, A.V. Kuznetsov, G.A. Salishchev, G.I. Raab, R.Z. Valiev, Effect of cold rolling on microstructure and mechanical properties of copper subjected to ECAP with various numbers of passes, Mater. Sci. Eng. A 554 (2012) 105-115.

[18] S. Sabbaghianrad, T.G. Langdon, A critical evaluation of the processing of an aluminum 7075 alloy using a combination of ECAP and HPT, Mater. Sci. Eng. A 596 (2014) 52-58.

[19] V.V Stolyarov, Y.T Zhu, T.C. Lowe, R.K Islamgaliev, R.Z Valiev, A two step SPD processing of ultrafine-grained titanium, Nanostruct. Mater. 11 (1999) 947-954.

[20] V.V. Stolyarov, Y.T. Zhu, T.C. Lowe, R.Z. Valiev, Microstructure and properties of pure Ti processed by ECAP and cold extrusion, Mater. Sci. Eng. A 303 (2001) 82-89.

[21] V.V. Stolyarov, Y.T. Zhu, I.V. Alexandrov, T.C. Lowe, R.Z. Valiev, Grain refinement and properties of pure Ti processed by warm ECAP and cold rolling, Mater. Sci. Eng. A 343 (2003) 43-50.

[22] A.P. Zhilyaev, B.-K. Kim, J.A. Szpunar, M.D. Baró, T.G. Langdon, The microstructural characteristics of ultrafine-grained nickel, Mater. Sci. Eng. A 391 (2005) 377-389.

[23] N. Lugo, N. Llorca, J.M. Cabrera, Z. Horita, Microstructures and mechanical properties of pure copper deformed severely by equal-channel angular pressing and high pressure torsion, Mater. Sci. Eng. A 477 (2008) 366-371.

[24] H.-J. Lee, S.K. Lee, K.H. Jung, G.A. Lee, B. Ahn, M. Kawasaki, T.G. Langdon, Evolution in hardness and texture of a ZK60A magnesium alloy processed by high-pressure torsion, Mater. Sci. Eng. A 630 (2015) 90-98.

[25] S. Sabbaghianrad, T.G. Langdon, An evaluation of the saturation hardness in an ultrafine-grained aluminum 7075 alloy processed using different techniques, J. Mater. Sci. 50 (2015) 4357-4365.

[26] S. Sabbaghianrad, T.G. Langdon, Microstructural saturation, hardness stability and superplasticity in ultrafine-grained metals processed by a combination of severe plastic deformation techniques, Lett. Mater. 5 (2015) 335-340.

[27] P. Bazarnik, B. Romelczyk, M. Kulczyk, M. Lewandowska, The strength and ductility of 5483 aluminium alloy processed by various SPD methods, Mater. Sci. Forum 765 (2013) 423-428.

[28] M. Furukawa, Z. Horita, M. Nemoto, R.Z. Valiev, T.G. Langdon, Microhardness measurements and the Hall-Petch relationship in an Al-Mg alloy with submicrometer grain size, Acta Mater. 44 (1996) 4619-4629.

[29] R.Z. Valiev, N.A. Enikeev, M.Yu. Murashkin, V.U. Kazykhanov, X. Sauvage, On the origin of the extremely high strength of ultrafine-grained Al alloys produced by severe plastic deformation, Scr. Mater. 63 (2010) 949-952.

[30] P. Bazarnik, Y. Huang, M. Lewandowska, T.G. Langdon, Structural impact on the Hall-Petch relationship in an Al-5Mg alloy processed by high-pressure torsion, Mater. Sci. Eng. A 626 (2015) 9-15.

[31] H.-J. Lee, J.-K. Han, S. Janakiraman, B. Ahn, T.G. Langdon, Significance of grain refinement on microstructure and mechanical properties of an Al-3% Mg alloy processed by high-pressure torsion, J. Alloy. Compd. 686 (2016) 998-1007.

[32] E.N. Popova, V.V. Popov, E.P. Romanov, V.P. Pilyugin, Thermal stability of nanocrystalline Nb produced by severe plastic deformation, Phys. Met. Metallogr. 101 (2006) 52-57.

[33] R.B. Figueiredo, P.H.R. Pereira, M.T.P. Aguilar, P.R. Cetlin, T.G. Langdon, Using finite element modeling to examine the temperature distribution in quasi-constrained high-pressure torsion, Acta Mater. 60 (2012) 3190-3198.

[34] R.Z. Valiev, Yu.V. Ivanisenko, E.F. Rauch, B. Baudelet, Structure and deformaton behaviour of Armco iron subjected to severe plastic deformation, Acta Mater. 44 (1996) 4705-4712.

[35] M. Andrzejczuk, J. Siejka-Kulczyk, M. Lewandowska, K.J. Kurzydłowski, Microstructure investigations of dental composite samples prepared by focused ion beam technique, J. Microsc. 237 (2010) 427-430.

[36] M. Kawasaki, R.B. Figueiredo, T.G. Langdon, An investigation of hardness homogeneity throughout disks processed by high-pressure torsion, Acta Mater. 59 (2011) 308-316.

[37] M. Kawasaki, J. Foissey, T.G. Langdon, Development of hardness homogeneity and superplastic behavior in an aluminum–copper eutectic alloy processed by high-pressure torsion, Mater. Sci. Eng. A 561 (2013) 118-125.

[38] M. Kawasaki, B. Ahn, T.G. Langdon, Significance of strain reversals in a two-phase alloy processed by high-pressure torsion, Mater. Sci. Eng. A 527 (2010) 7008-7016.

[39] M. Kawasaki, Different models of hardness evolution in ultrafine-grained materials processed by high-pressure torsion, J. Mater. Sci. 49 (2014) 18-34.

[40] S. Sabbaghianrad, J. Wongsa-Ngam, M. Kawasaki, T.G. Langdon, An examination of the saturation microstructures achieved in ultrafine-grained metals processed by high-pressure torsion, J. Mater. Res. Technol. 3 (2014) 319-326.

[41] E.O. Hall, The deformation and ageing of mild steel III Discussion of results, Proc. Phys. Soc. Sect. B 64 (1951) 747-753.

[42] N.J. Petch, The cleavage strength of polycrystals, J. Iron Steel Inst. 174 (1953) 25–28.

[43] D.A. Hughes, N. Hansen, Microstructure and strength of nickel at large strains, Acta Mater. 48 (2000) 2985-3004.

[44] N. Hansen, Hall-Petch relation and boundary strengthening, Scripta Mater. 51 (2004) 801-806.

[45] H.W. Zhang, K. Lu, R. Pippan, X. Huang, N. Hansen, Enhancement of strength and stability of nanostructured Ni by small amounts of solutes, Scripta Mater. 65 (2011) 481-484.

[46] Q. Liu, X. Huang, D.J. Lloyd, N. Hansen, Microstructure and strength of commercial purity aluminium (AA 1200) cold-rolled to large strains, Acta Mater. 50 (2002) 3789-3802.

[47] N. Balasubramanian, T.G. Langdon, The strength–grain size relationship in ultrafine-grained metals, Metall. Mater. Trans. A 47A (2016) 5827–5838.

[48] R.W. Armstrong, N. Balusubramanian, Unified Hall-Petch description of nano-grain nickel hardness, flow stress and strain rate sensitivity, AIP Adv. 7 (2017) 085010(1-5).

Figure captions

Fig. 1 Bright field TEM images and SAED patterns of aluminium 5483 alloy after HE processing showing microstructure diversification: (a) region with undeformed coarse grains, (b) region with intense grain refinement, (c) cross-sectional image showing fibrous morphology.

Fig. 2 Representative bright field images in TEM with the corresponding SAED patterns showing the microstructure in the centre and edge of the samples processed by a combination of HE and HPT through (a,e) 1/2, (b,f) 1, (c,g) 5 and (d,h) 10 revolutions.

Fig. 3 Bright field TEM images from the cross-sectional plane near the centre of the disk supplemented with SAED patterns taken from the sample processed by a combination of HE and 1/4 turn of HPT.

Fig. 4 Distribution of the number fractions of the misorientation angles of the grain boundaries of disks processed by HE and by 1/2, 1, 5 and 10 turns of HPT.

Fig. 5 Values of Vickers microhardness across diameters of the disks for HE and a combination of HE and various numbers of turns in HPT; the lower dashed line shows the as-annealed condition.

Fig. 6 The average Vickers microhardness values after processing only by HPT [30] and for a combination of HE and various numbers of turns in HPT

Fig. 7 Variation of Vickers microhardness plotted against the equivalent strain after processing (a) by HE and a combination of HE and various numbers of turns in HPT, (b) by HPT based on data reported in an earlier investigation [30].

Fig. 8 The Hall-Petch relationship for samples processed by a combination of HE and various numbers of turns of HPT; data also includes experimental points for samples processed only by HPT [30] and experimental points for the alloy with larger coarse grain sizes [11,27,30]

Table captions

Table 1 Microstructural parameters for the aluminium 5483 alloy after HPT [30] and HE+HPT processing depending on the number of turns.

Table 2 HAGBs fraction and average GB misorientation angles in aluminium 5483 alloy after HPT [30] and HE + HPT depending on the number of turns.

Table 1 Microstructural parameters for the aluminium 5483 alloy after HPT [30] and HE+HPT processing depending on the number of turns.

	Number of turns	1/4	1/2	1	3	5	7	10
HE+HPT	Average grain size [nm]	150	164	132	120	111	80	61
	Standard deviation	61	78	52	67	55	35	24
HPT	Average grain size [nm]	175	155	137	113	105	93	79
	Standard deviation	122	96	81	89	64	46	30

Table 2 HAGBs fraction and average GB misorientation angle in aluminium 5483 alloy after HPT [30] and HE + HPT depending on the number of turns.

Number of turns	HE+HPT		HPT [30]	
	E(θ)	Fraction of HAGB [%]	E(θ)	Fraction of HAGB [%]
N = 1/2	28.7°	71.1	22.3°	54.4
N = 1	32.8°	81.9	34.7°	69.5
N = 5	34.1°	84.4	31.6°	75.7
N = 10	38.2°	93.6	35.9°	80.6

Figure 1

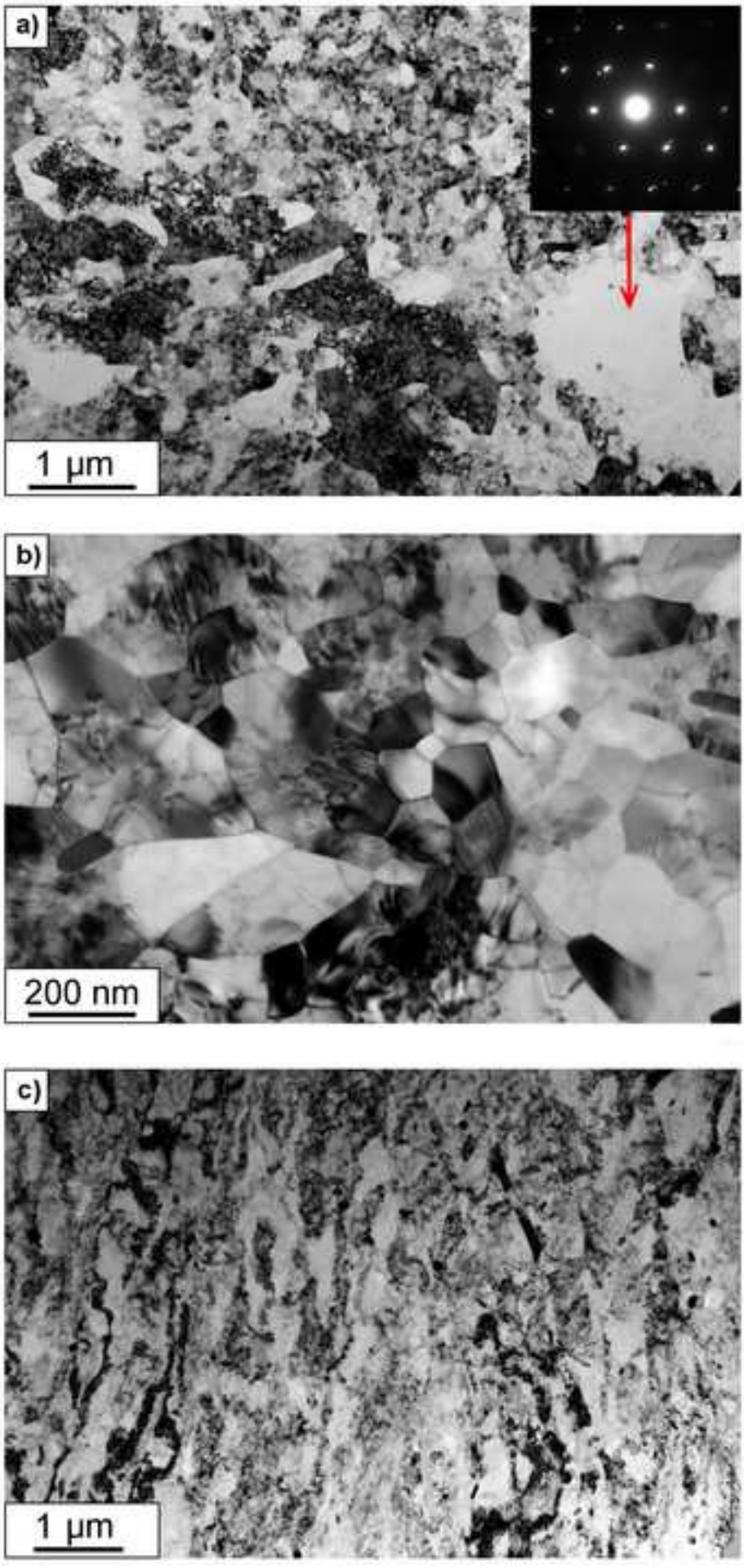

Figure 2

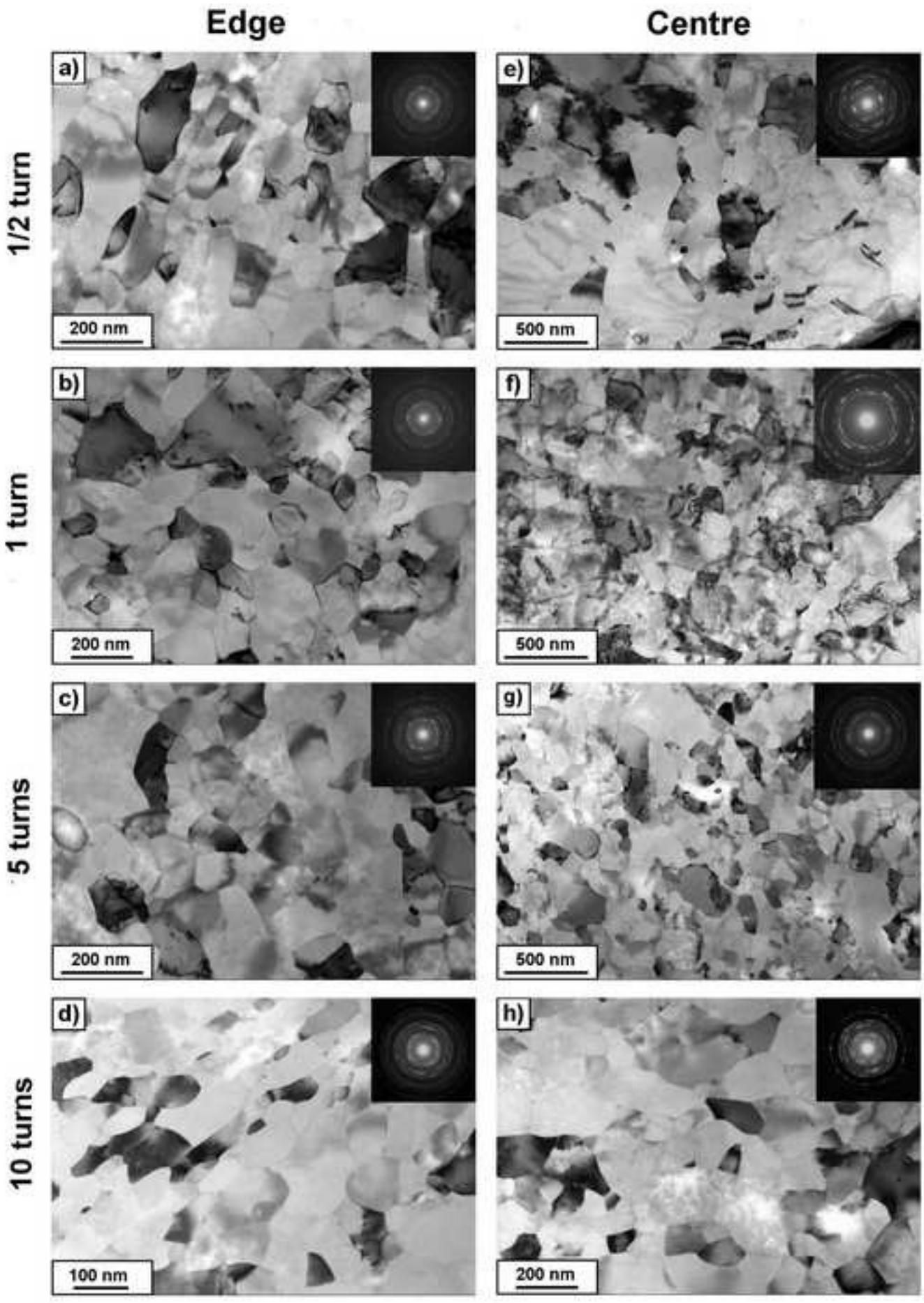

Figure 3

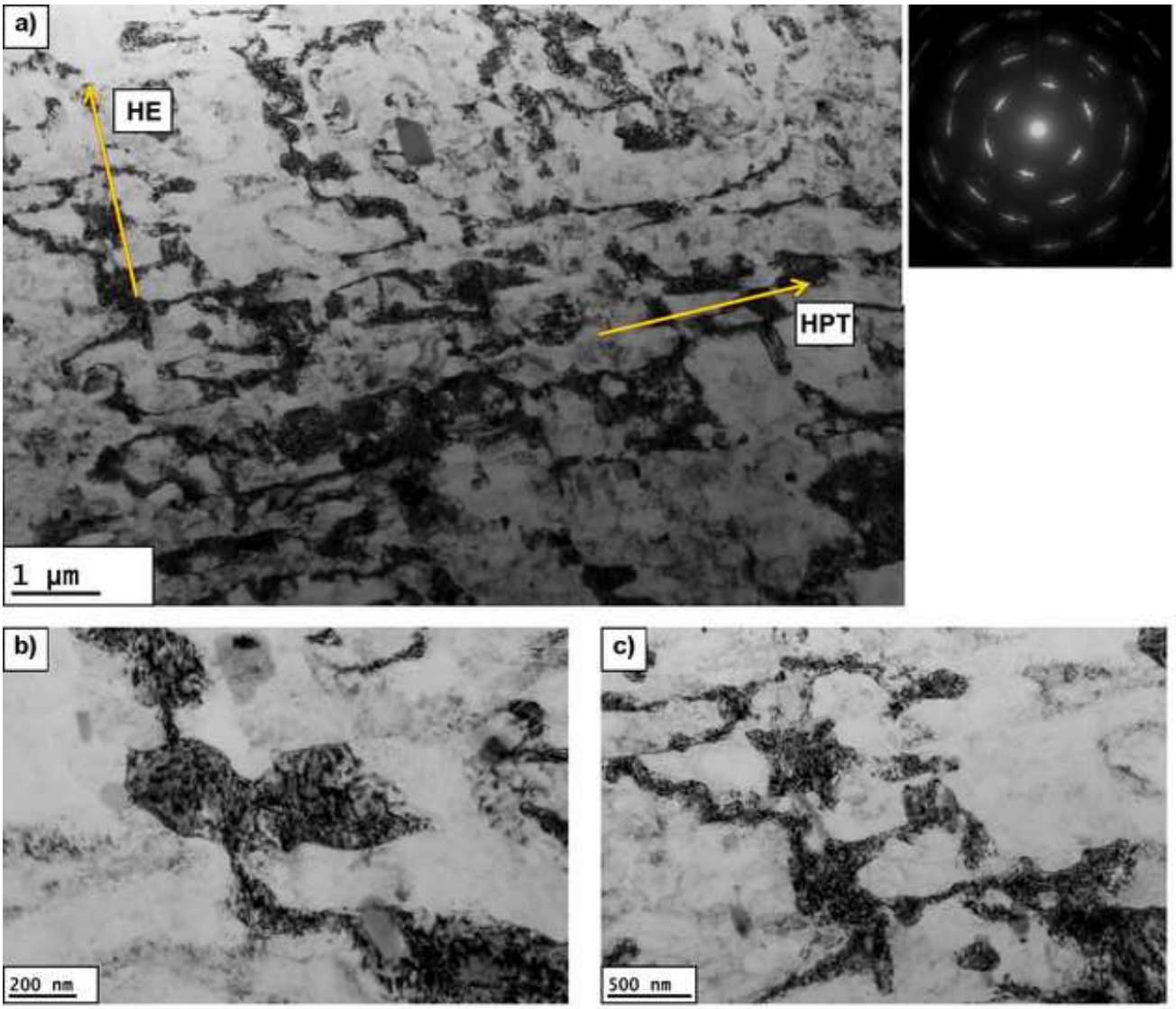

Figure 4

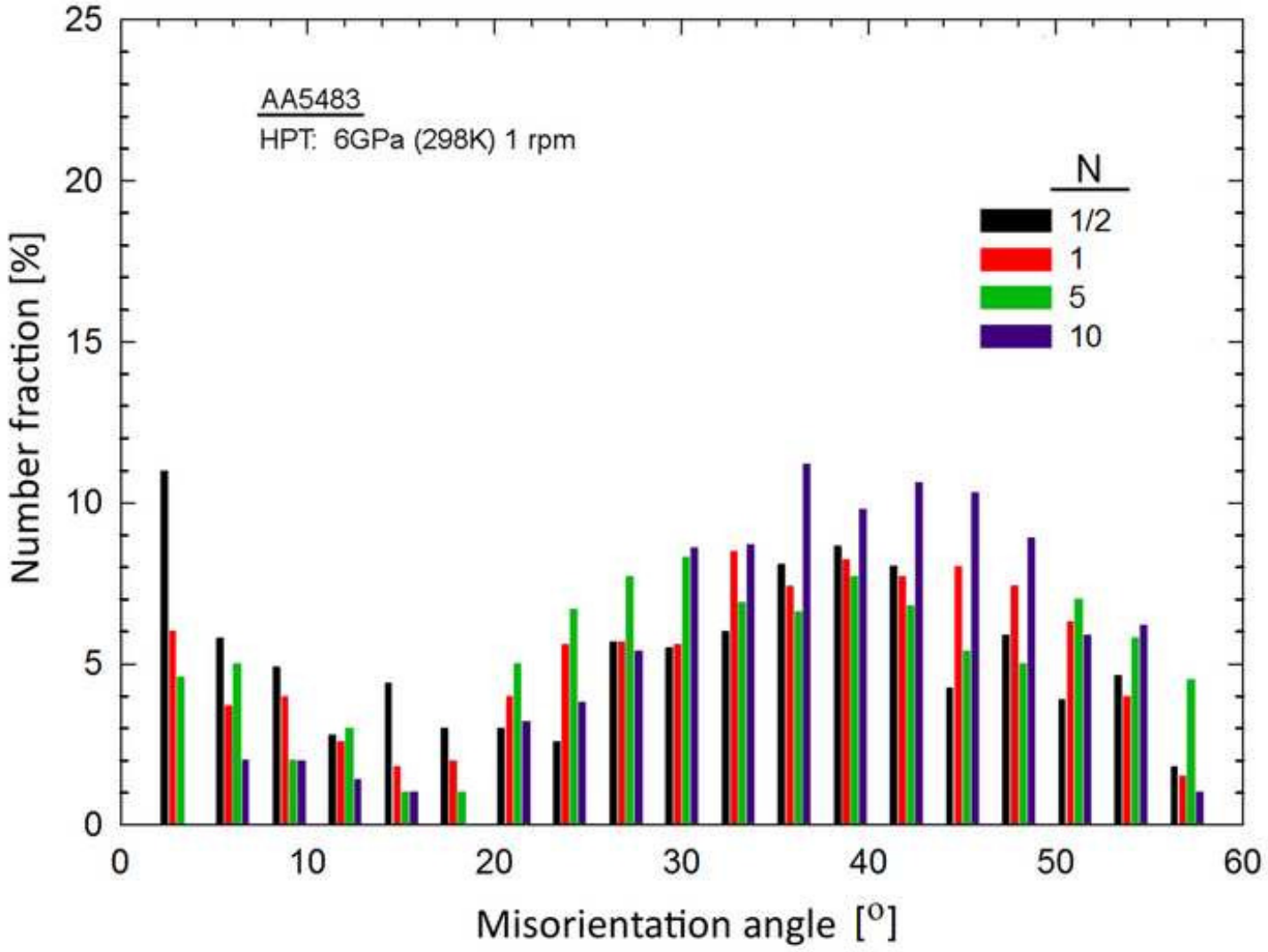

Figure 5

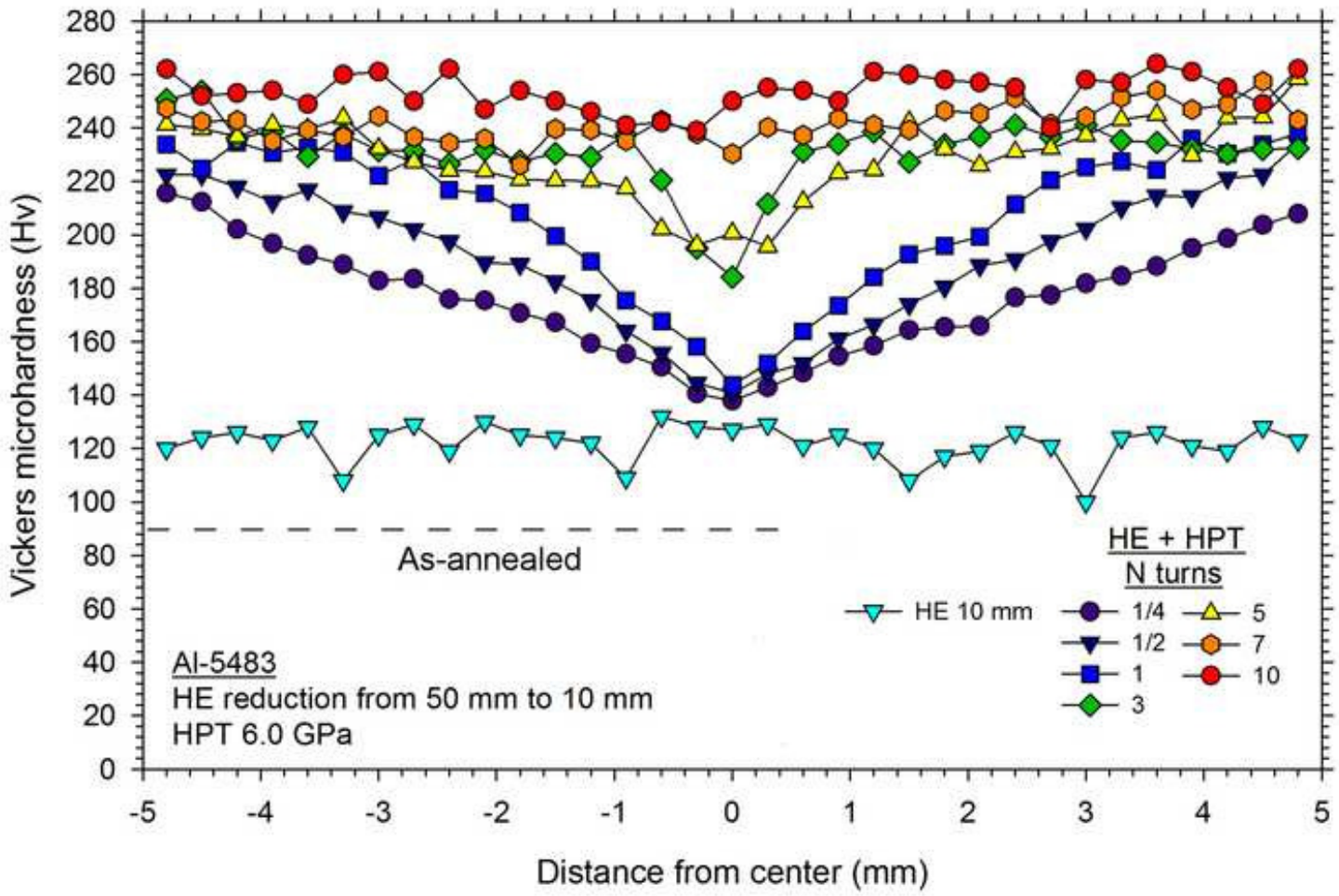
Vickers microhardness (Hv)
Distance from center (mm)
As-annealed
Al-5483
HE reduction from 50 mm to 10 mm
HPT 6.0 GPa
HE + HPT
N turns
HE 10 mm
1/4
1/2
1
3
5
7
10

Figure 6

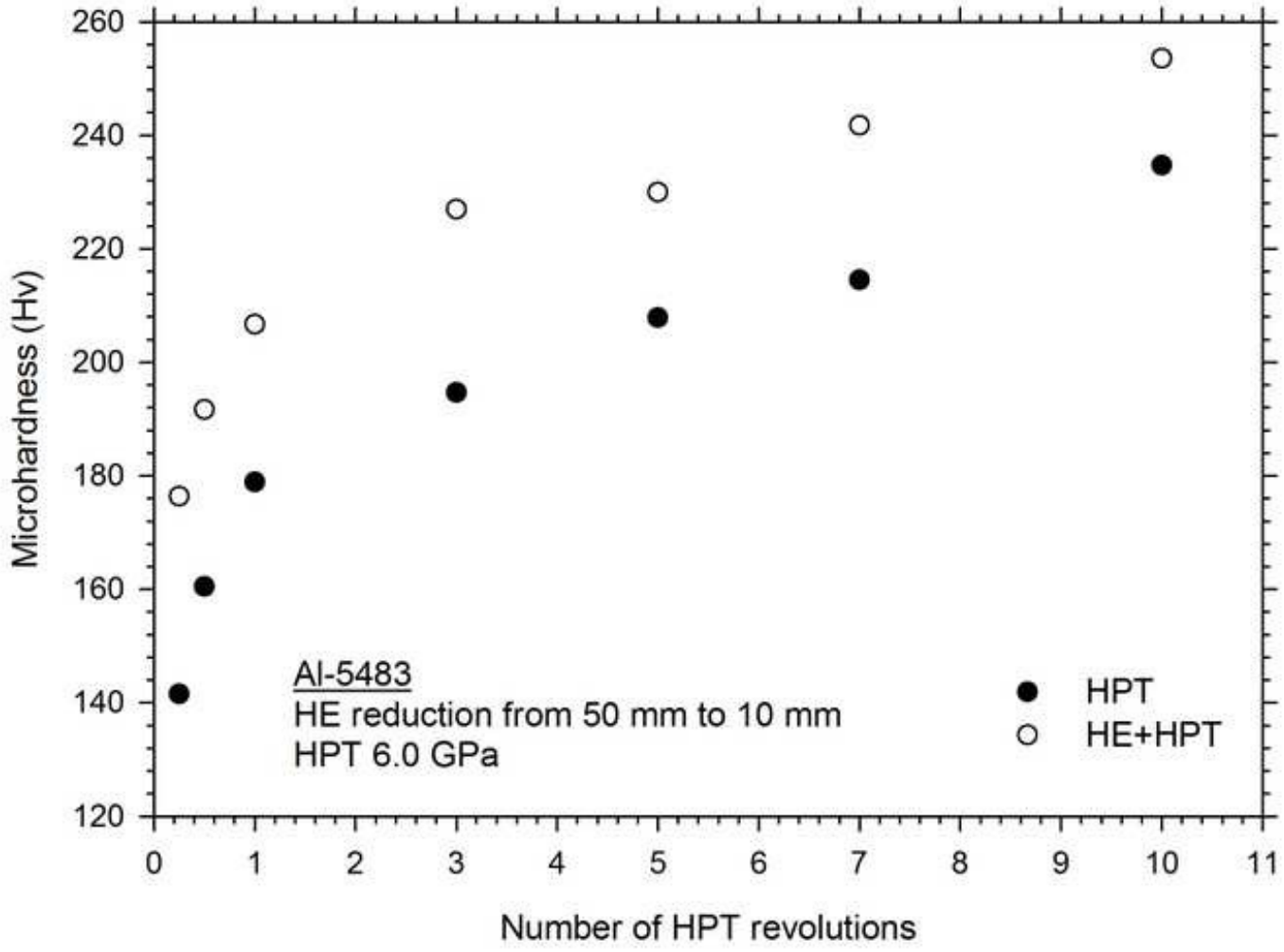

Figure 7

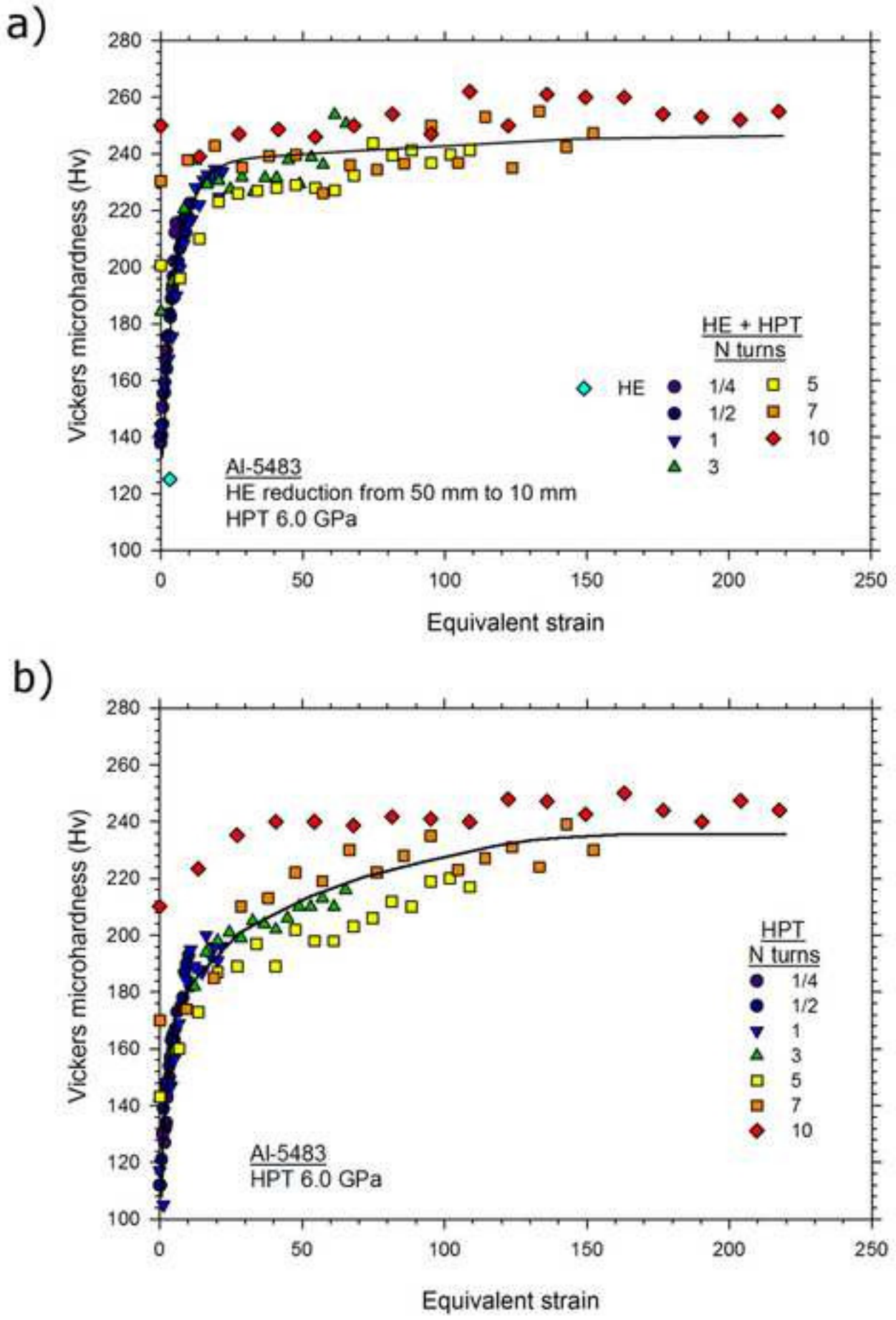

Figure 8